New C_{2v}- and Chiral C_2-Symmetric Olefin Polymerization Catalysts Based on Nickel(II) and Palladium(II) Diimine Complexes Bearing 2,6-Diphenyl Aniline Moieties: Synthesis, Structural Characterization, and First Insight into Polymerization Properties

Markus Schmid,[†] Robert Eberhardt,[†] Martti Klinga,[‡] Markku Leskelä,[‡] and Bernhard Rieger*[,†]

Department of Materials and Catalysis, University of Ulm, D-89069 Ulm, Germany, and Department of Chemistry, University of Helsinki, FIN-00014 Helsinki, Finland[1]

Received January 2, 2001

Four new 1,4-diaza-2,3-dimethylbutadiene ligands (Ar−N═C(CH_3)−(H_3C)C═NAr; Ar: **3a** = 2,6-diphenylphenyl; **3b** = 2,6-di(4-OCH_3-phenyl)phenyl; **3c** = 2,6-di(4-*tert*-butyl-phenyl)-phenyl; **3d** = 2,6-di(3,5-dimethylphenyl)phenyl) as well as the palladium dichloride complexes **4a**−**c** and methyl monochloride derivatives **5a**−**c** were prepared, and their polymerization behavior was investigated. The corresponding nickel species **6a**−**c** were tested for the insertion polymerization of ethene by in situ reactions of **3a**−**c** with (DME)$NiBr_2$. The ligands are accessible by a three-step procedure. Aryl boronic acids were prepared by Grignard reactions of substituted aryl bromides and were coupled with 2,6-dibromo aniline according to a Suzuki cross-coupling protocol to give the corresponding terphenyl anilines **2a**−**d**. Condensation of 2,3-butanedione with the corresponding aniline afforded the formation of the diimines **3a**−**d**. The corresponding palladium dichloride complexes **4a**−**c** are accessible by reaction with $(PhCN)_2PdCl_2$. The structures of **4a**−**c** could be determined by X-ray analysis. While the terphenyl complex **4a** adopts a C_{2v}-symmetry, **4c** exists in a chiral C_2-symmetric coordination geometry, due to the repulsive interactions of the sterically demanding *tert*-butylphenyl substituents of the aniline moieties. All palladium and nickel complexes are catalysts for the polymerization of ethene. However, the chiral Ni(II) complex **6c** shows by far the highest polymerization activity up to 2×10^4 kg(PE) [mol (Ni) h]$^{-1}$. The polyethenes obtained with the palladium methyl monochloro catalysts activated with Na-[(3,5-$(CF_3)_2C_6H_3)_4$B] and the nickel dibromo complexes activated with MAO are linear and show in the case of the Ni(II) derivatives molecular weights up to 4.5×10^6 g mol^{-1} ($M_w/M_n \approx 2$), which can be controlled by addition of hydrogen.

Introduction

Early transition metal d^0-complexes such as single-site zirconocene catalysts are extensively used for the coordination polymerization of apolar 1-olefins such as ethene and propene.[2] These complexes are difficult to handle and incompatible with polar monomers due to the high Lewis acidity and oxophilicity of the polymerization active monocations. Recently, intensive research activities have been focused on late transition metal complexes as polymerization catalysts, although they often only dimerize or oligomerize 1-olefins due to competing β-hydride elimination reactions.[3]

Following the pioneering studies of Keim[3] and Fink[3] in the 1970s and 1980s, mainly Brookhart and co-workers have reported on the development of palladium-(II) and nickel(II) diimine complexes (Chart 1) that polymerize ethene to high molecular weight polymers comprising a branched microstructure.[4] The steric demand of the bulky isopropyl substituents on the aniline moieties and their orientation toward the virtual apical positions of the square-planar complexes is crucial for an optimal alignment of the incoming monomer relative to the growing polymer chain. It obviously blocks associative olefin exchange and effectively retards chain transfer.[5]

The present contribution reports on a series of new diimine ligands and complexes bearing 2,6-diphenyl-

[†] University of Ulm.
[‡] University of Helsinki.
(1) **4a**, **4c** X-ray diffraction.
(2) Coats, G. W.; Waymouth, R. M. *Science* **1995**, 267, 217. (b) Wang, X.; Stern, C. L.; Marks, T. J. *J. Am. Chem. Soc.* **1994**, *116*, 10015. (c) Crowther, D. J.; Baenziger, N. C.; Jordan, R. F. *J. Am. Chem. Soc.* **1991**, *113*, 1455. (d) Kaminsky, W.; Külper, K.; Brinzinger, H. H.; Wild, F. R. W. P. *Angew. Chem., Int. Ed. Engl.* **1985**, *24*, 507.
(3) Rix, F.; Brookhart, M. *J. Am. Chem. Soc.* **1995**, *117*, 1137. (b) Peuckert, M.; Keim, W. *Organometallics* **1983**, *2*, 594. (c) Wilke, G. *Angew, Chem,. Int. Ed. Engl.* **1988**, *27*, 185.
(4) Johnson, L. K.; Killian, C. M.; Brookhart, M. *J. Am. Chem. Soc.* **1995**, *117*, 6414. (b) Pappalardo, D.; Mazzeo, M.; Pellecchia, C. *Macromol. Rapid Commun.* **1997**, *18*, 1017.
(5) Johnson, L. K.; Mecking, S.; Brookhart, M. *J. Am. Chem. Soc.* **1996**, *118*, 267. (b) Ittel, S. D.; Johnson, L. K.; Brookhart, M. *Chem. Rev.* **2000**, *100*, 1169. (c) Britovsek, G. J. P.; Gibson, V. C.; Wass, D. F. *Angew. Chem.* **1999**, *111*, 448.

10.1021/om010001f CCC: $20.00
Publication on Web 05/01/2001

Chart 1

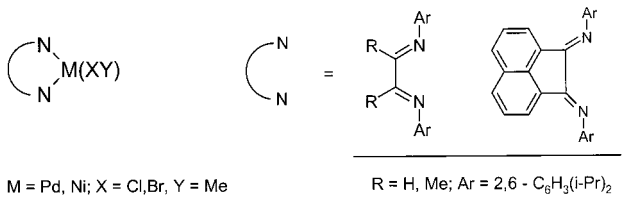

Chart 2

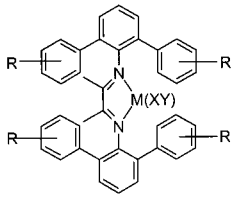

a: R = H
b: R = 4-methoxy
c: R = 4-*t*-butyl
d: R = 3,5-dimethyl

4: M = Pd; X = Y =Cl
5: M = Pd; X = Cl, Y = Me
6: M = Ni; X = Y = Br

modified aniline moieties (Chart 2). Our concept aims to maintain the steric demand of the substituents in 2,6-position but allows a further easy modification of the steric and electronic properties of the polymerization active species. To develop this novel catalyst generation also toward potentially stereoselective polymerization reactions, one major perspective was the synthesis of the 2,6-bis(4-*tert*-butylphenyl)aniline building block. The diimine ligand derived thereof was expected to adopt spontaneously a chiral, C_2-symmetric coordination geometry around the metal center, due to repulsive steric interactions of adjacent *tert*-butyl groups.

Results and Discussion

Ligand and Complex Synthesis. Brookhart's diimine ligands can be obtained by a simple condensation reaction of α,*β*-diketones with commercially available 2,6-diisopropyl aniline.[6] An efficient strategy to access the 2,6-diphenyl-substituted anilines of the present work is the palladium-catalyzed cross-coupling of aryl boronic acids with aryl bromides (Scheme 1). Mild reaction conditions, a high selectivity as well as good yields, and the tolerance against functional groups made this method convenient for us.[7] The aryl boronic acids **1a**−**d** can easily be synthesized by treatment of the corresponding aryl Grignard compounds with trimethylborate.[8]

The Suzuki reactions were performed via a single-pot protocol by modifying a literature procedure of Miura.[9] The lavish workup by column chromatography was substituted by precipitating the amines as hydro chloride or hydro bromide salts by addition of the corresponding hydro halogenic acid to the organic layer. The pure anilines **2a**−**d** could be isolated from diethyl ether after neutralization with aqueous Na_2CO_3 solution. The terphenyl diimine ligands **3a**−**d** were subsequently prepared by refluxing a solution of 2,3-butanedione and the amino compound in benzene under the catalytic influence of *p*-toluene sulfonic acid. Longer reaction times had to be applied with increasing steric demand of the *p*-substituents to isolate the products in satisfying to good yields (61−85%).

Complexes **4a** and **5a** are accessible by reaction of **3a** with the respective CODPd(II)Cl_2 precursor in toluene at ambient temperature.[10] The substituted terphenyl ligands **3b**,**c** are unable to displace the COD fragment effectively. Satisfying results were obtained by using $(C_6H_5CN)_2PdCl_2$ as starting material.[11] Subsequent treatment of the dichloro complexes **4a**−**c** with $Sn(CH_3)_4$ afforded the monomethyl compounds **5b**,**c** (Scheme 2).[12]

Solid State Structures. The structures of the palladium dichloro compounds **4a**−**c** could be determined by single-crystal X-ray analysis. Compounds **4a**,**c** show disorder, which could be resolved satisfactorily. The expected bidentate coordination of the diimine nitrogen atoms to the Pd(II) center, forming square-planar (Figure 1a,b) and distorted square-planar (Figure 1c) coordination environments, is found for all three complexes. Table 1 summarizes the most relevant bonding parameters. The crystal, intensity collection, and refinement data for compounds **4a**−**c** are presented in Table 2.

The phenyl substituents are found in the 2,6-positions of the aniline moieties, as expected. These phenyl rings point toward each other above and below the N−Pd−N plane as a consequence of this specific location. In **4a**, each terphenyl moiety is not large enough to feel the steric influence of its symmetry-related counterpart, leading to a nearly ideal C_{2v}-symmetry. However, already here, the aniline-phenyl groups cannot rotate freely around their N−C_{arom} bond, as checked by variable-temperature NMR experiments up to 100 °C.[13] Introduction of the 4-methoxy (**4b**, Figure 1b) and 4-*tert*-butyl substituents (**4c**, Figure 1c) leads to a situation where repulsive interactions between the fragments pointing toward each other become relevant. This effect is already present in **4b**, although the oxygen atoms allow the methyl groups to rotate and point away from each other, limiting structural consequences. This is clearly different for the *tert*-butyl groups in **4c**. The racemic complex species adopts a chiral, C_2-symmetric coordination geometry, due to the distinct repulsion of the *tert*-butyl fragments. To give a more quantitative description of the influence of the 2,6-diphenyl substitutents, we introduce the following definition of the angles ϵ, ϕ, and λ, describing the orientation of the phenyl group planes relative to each other (Chart 3).

The planes A, B, and C (A′, B′, C′, respectively) as well as the corresponding plane vectors were calculated by least-squares methods using the corresponding X-ray data. ϵ is defined as the angle between the vectors $\vec{\chi}_1$

(6) Dieck, H. t.; Svoboda, M.; Greiser, T. *Z. Naturforsch. B: Chem. Sci.* **1981**, *36*, 823. (b) Van Asselt, R.; Gielens E. E. C. G.; Rülke, R. E.; Vrieze, K. *J. Am. Chem. Soc.* **1994**, *116*, 977.

(7) Miyaura, N.; Yanagi, T.; Suzuki, A. *Synth. Commun.* **1981**, *11*, 513. (b) Miyaura, N.; Suzuki, A. *Chem. Rev.* **1995**, *95*, 2457. (c) Martin, A. R.; Yang, Y. *Acta Chem. Scand.* **1993**, *47*, 221.

(8) Bowie, R. A.; Musgrave, O. C. *J. Chem. Soc. (C)* **1966**, 566.

(9) Miura, Y.; Oka, H.; Momoki, M. *Synthesis* **1995**, 1419.

(10) Nagel, U.; Rieger, B. *Chem. Ber.* **1988**, *121*, 1123.

(11) v. Asselt, R.; Elsevier, C. J.; Amatore, C.; Jutland, A. *Organometallics* **1997**, *16*, 316.

(12) Lapido, F. T.; Anderson, G. K. *Organometallics* **1994**, *13*, 303.

(13) We checked the inability of the terphenyl system to rotate even at elevated temperatures also experimentally: the compound bis(2-phenyl)anilinediaminePdCl_2 shows two diastereoisomers (rac and meso) in the NMR up to 100 °C. Also here, with only one phenyl substituent in the 2-position, no free rotation occurs. If instead of the 2-phenyl aniline moiety, a 1-aminotetrahydronaphthaline residue is introduced, showing a more constrained substitution, no diastereoisomers can be detected, indicating free rotation around the N−C_{arom} bond already at room temperature.

Scheme 1

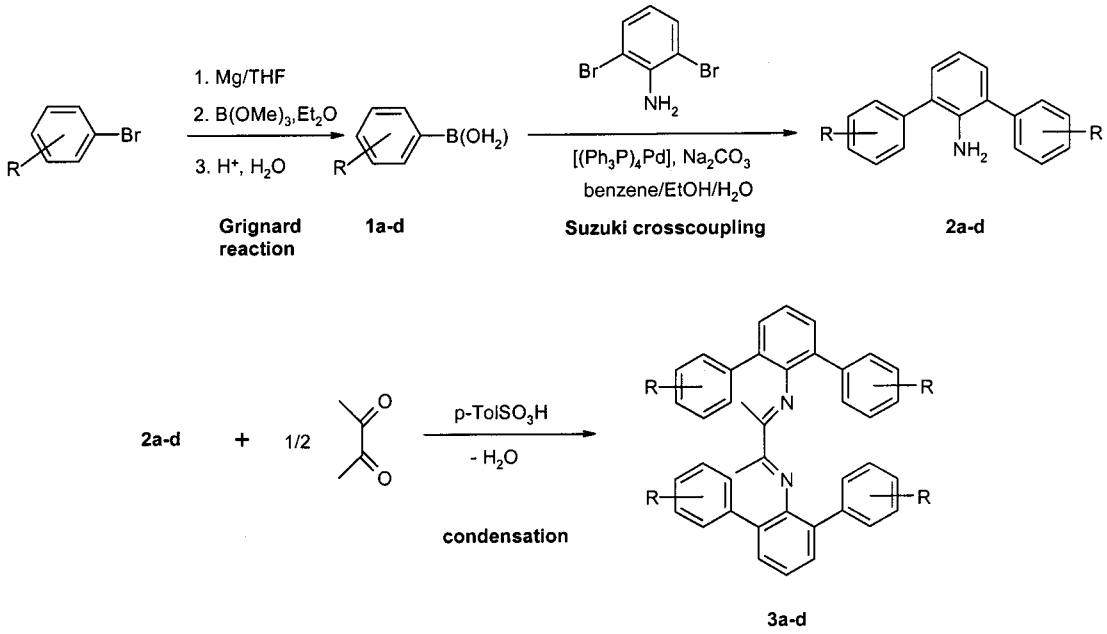

Scheme 2

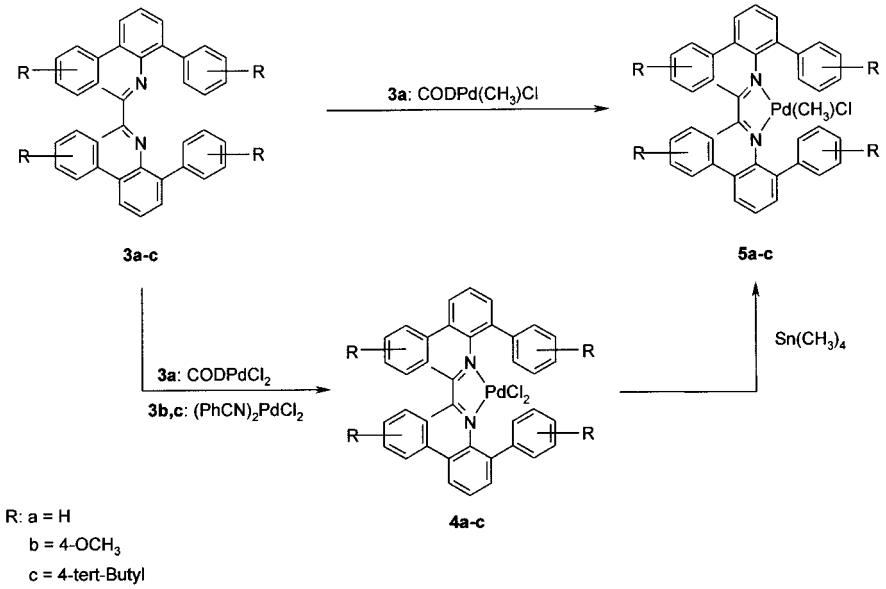

and $\vec{\chi}_2$. ϕ describes the level of distortion of the "terphenyl wings" and is given as the angle between the plane vectors $\vec{E}_A$ and $\vec{E}_{A'}$. λ is a measure of the staggered arrangement of the phenyl planes B and C within one "terphenyl wing" and is defined as the angle between the plane vectors $\vec{E}_B$ and $\vec{E}_C$.

ϕ is 7.5° for the terphenyl complex **4a**, indicating that there is almost no distortion, as expected from the above discussion. ϕ increases to 27.8° by introduction of the 4-methoxy groups in **4b**, and the structure begins to avoid the steric influence of the *para*-groups by adopting a distorted conformation in the crystalline state. If the steric demand of the 2,6-diphenyl substituents is increased by exchanging the 4-methoxy groups by *tert*-butyl fragments (**4c**), ϕ is increased to 51.4° and the structure is finally tipped over into a distinct chiral, C_2-symmetric geometry (Figure 1c, 2). The two substitutents pointing toward the Pd(II) atom push the chloride atoms down (or up, respectively), so that the metal ion is forced to give up its favored square-planar coordination environment. The same steric influence of the rear pointing 2-(4-*tert*-butyl)phenyl groups on the methyl substituents of the backbone forces the metallacycle to adopt a chiral conformation, too.

The cones defined by the ϵ-angles can be regarded as an indication of the steric shielding of the metal center with respect to the virtual apical positions of the coordination polyhedron. The ϵ-values are practically identical for **4a**,**b** (Chart 3: 127.0°, 125.6°, respectively). Interestingly, this angle is significantly increased to 138.6° in **4c**. We attribute this effect again to the strong repulsive interaction between the 2-(4-*tert*-butyl)phenyl fragments (Figure 1c).

Also the planes of the phenyl groups in 2,6-position of the aniline moiety form pairwise chiral elements, which becomes obvious by inspection of the top view of the molecules (Chart 3). While there is no significant change of λ for **4a**,**b** again, this angle decreases to

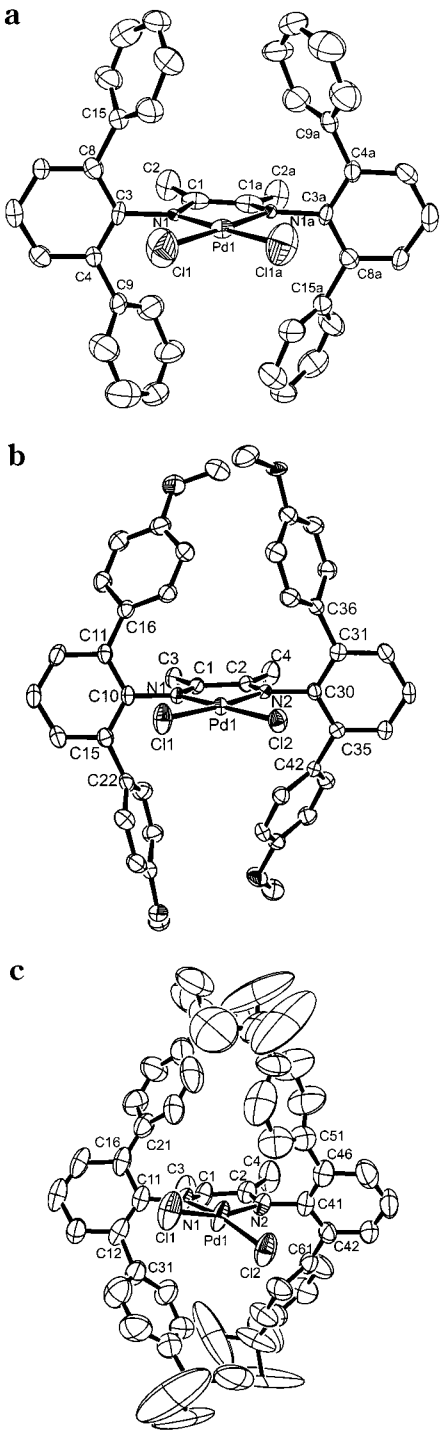

Figure 1. (a) ORTEP plot of complex **4a** showing the atom-labeling scheme; atoms labeled with "a" were generated by symmetry operations; thermal ellipsoids are depicted at a 50% probability level. Hydrogen atoms are omitted for clarity. (b) ORTEP plot of complex **4b** showing the atom-labeling scheme; thermal ellipsoids are depicted at a 50% probability level. Hydrogen atoms are omitted for clarity. (c) ORTEP plot of complex **4c** showing the atom-labeling scheme; thermal ellipsoids are depicted at a 50% probability level. Hydrogen atoms are omitted for clarity.

43.3° in complex **4c**, supporting further the stereorigid ligand arrangement there. However, no signals arising from diasteroisomers can be detected in solution, indicating that rotation is fast, at least on the NMR time scale.

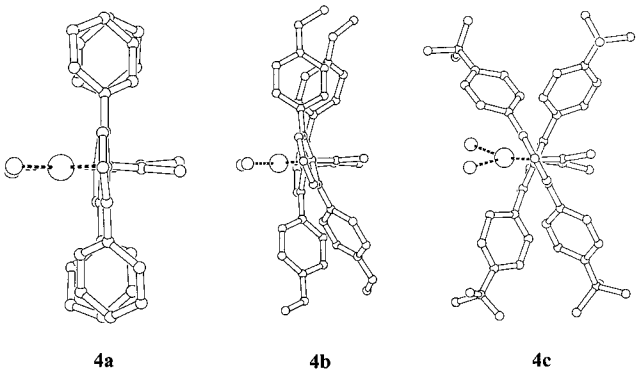

Figure 2. Influence of the *p*-substituents on the distortion angle ϕ. A strong increase in the angle ϕ was observed for enhancing the sterical demand of the groups in 4-positions.

Ethene Polymerization Experiments

Palladium Monomethyl Complexes. The polymerization reactions were performed in 50 and 100 mL steel autoclaves in 30 or 50 mL of CH_2Cl_2 at room temperature.[14] Two equivalents of $NaB(Ar')_4$ ($Ar' = 3,5\text{-}CF_3(C_6H_3)$) were added to activate **5a**−**c**. Remarkably, all three Pd(II) catalysts decomposed readily during the polymerization reaction. This observation was confirmed by recording the monomer consumption as a function of time. The gas flow faded within the first minutes and came to an end after 15−20 min. This fast decomposition occurs independent of the activation temperature (−78 °C or RT) and of the presence of monomer. At the moment we do not have a genuine explanation for this surprising instability.[15] However, it is obvious that the fast decomposition not only is the reason for the low polymer yields but also prevents the formation of higher molecular weight products (Table 3).

Nickel Dibromides 6a−c. The corresponding Ni(II) species **6a**−**c** were synthesized in situ[16] by reaction of $(DME)NiBr_2$ with the ligands **3a**−**c**. The activation was performed by treatment with MAO at ambient temperature in order to circumvent decomposition problems similar to those observed with **5a**−**c**/$NaB(Ar')_4$. **6a**−**c**/MAO are highly active catalysts for the polymerization of ethene (Table 4). The 2,6-diphenyl-substituted **6a**/MAO gives yields that are similar to those found for Brookhart's catalyst **6e**/MAO (Table 4, entries 1 and 6). The activities of **6a**−**c**/MAO increase substantially at higher monomer concentrations, exceeding those of **6e**/MAO considerably under our conditions. Surprisingly, the chiral complex **6c**/MAO shows by far the highest activities, which increase up to 2×10^4 g(PE) (mol(Ni) h)$^{-1}$ at 30 bar ethene pressure (Figure 3). We attribute this interesting effect to the *tert*-butyl-substituted aniline fragments. Their chiral arrangement guides the incom-

(14) For related work on 2,6-disubstituted aniline fragments cf. also Eastman Chemical Company, WO 00/50470.

(15) It might have to do with the particular activation protocol. This is supported by trials to activate the $PdCl_2$ species by treatment with MAO that failed. The only exception is **4c**, which showed some activity after reaction with MAO presumably due to the presence of four intramolecular ether fragments per palladium atom. A detailed investigation on this effect and on the polymerization properties of **4c** is right now underway.

(16) A series of experiments with different reaction times showed that the conversion was completed after stirring the reaction mixture overnight.

Table 1. Selected Bond Lenghts (Å) and Angles (deg) for 4a−c[a]

4a		4b		4c	
		Bond Lengths			
Pd1−N1	2.032(7)	Pd1−N1	2.034(4)	Pd1−N1	2.004(4)
Pd1−N1a	2.032(7)	Pd1−N2	2.022(4)	Pd1−N2	2.028(4)
Pd1−Cl1	2.205(5)	Pd1−Cl1	2.284(2)	Pd1−Cl1	2.2711(14)
Pd1−Cl1a	2.205(5)	Pd1−Cl2	2.298(1)	Pd1−Cl2	2.2363(16)
N1−C3	1.484(8)	N1−C10	1.460(6)	N1−C11	1.439(6)
		N2−C30	1.455(6)	N2−C41	1.411(6)
C1−C1a	1.482(10)	C1−C2	1.507(6)	C1−C2	1.463(7)
C1−C2	1.532(9)	C1−C3	1.484(6)	C1−C3	1.470(7)
		C2−C4	1.483(8)	C2−C4	1.493(7)
C1−N1	1.300(8)	C1−N1	1.286(6)	C1−N1	1.275(6)
		C2−N2	1.288(6)	C2−N2	1.280(6)
		Bond Angles			
N1−Pd1−N1a	78.9(4)	N1−Pd1−N2	79.0(2)	N1−Pd1−N2	79.73(15)
N1−Pd1−Cl1	98.0(3)	N1−Pd1−Cl1	95.9(1)	N1−Pd1−Cl1	95.43(11)
N1−Pd1−Cl1a	176.9(3)	N1−Pd1−Cl2	174.5(1)	N1−Pd1−Cl2	164.15(14)
N1a−Pd1−Cl1	176.9(3)	N2−Pd1−Cl1	174.2(1)	N2−Pd1−Cl1	165.82(14)
N1a−Pd1−Cl1a	98.0(3)	N2−Pd1−Cl2	95.9(1)	N2−Pd1−Cl2	95.64(11)
Cl1−Pd1−Cl1a	85.2(4)	Cl1−Pd1−Cl2	89.3(1)	Cl1−Pd1−Cl2	92.40(6)

[a] Symmetry transformations used to generate equivalent atoms in **4a**: (a) $-x+2, -y, z$.

ing monomer effectively into the optimal coordination position on the Ni(II) center and helps to suppress 2,1-reinsertions after β-hydride abstraction from the growing chain. This reduces the propability of the formation of secondary Pd−C bonds (cf. discussion of product linearity below)[17] that show a notably lower reaction rate toward the next incoming monomer compared to their primary analogues. The low activity of **6b**/MAO (entry 5) results clearly from a reaction with MAO (probably through coordination via the methoxy units), indicated by the formation of an insoluble precipitate directly after MAO addition.

The molecular weight of the polyethenes produced under these conditions exceeds 4.5×10^6 g mol^{-1}, which is the limit of our HT GPC setup and could thus be determined only in one case (Table 4, entry 3). However, DSC measurements—also in comparison of products formed with **6e**/MAO (Table 4, entry 6)—demonstrated the linear character of the ultrahigh molecular weight polyethenes, prepared with **6a**−**c**/MAO (Table 4, $T_m \geq$ 130 °C). An obvious reason for the linearity of our polyethenes that results from catalysts with high steric demand comes from quantum mechanical considerations recently performed on Ni, Pd(II) diimine complexes.[18] Ziegler and co-workers suggested that the formation of branches requires a rotation of the vinyl chain end resulting from β-hydride elimination before a 2,1-reinsertion can occur. The rate of such a rotation should be reduced with increasing steric demand of the ligand system, leading to more linear products with increased molecular weight. The same argumentation was used to explain the linearity of the polyethenes resulting from Fe^{II}- and Co^{II}-bisimino(pyridine) complexes and might also be accepted as true for complexes such as **6a**,**c**.[19] The molecular weight of the polymer products can be effectively controlled by the addition of hydrogen. M_w could be varied from 2×10^5 to 1×10^6 g mol^{-1} under different H_2 concentrations using **6c**/MAO (Table 5). Hydrogen does not seem to reduce and thus to inactivate the Ni(II) catalysts (Figure 4). In contrast, the activity increases significantly with the addition of H_2. A reasonable explanation for this unexpected effect might be the more homogeneous reaction conditions, but also a fast hydrogenation of less reactive intermediates, like those resulting from 2,1-insertions. The melting points attest to the highly crystalline character of the polyethenes.

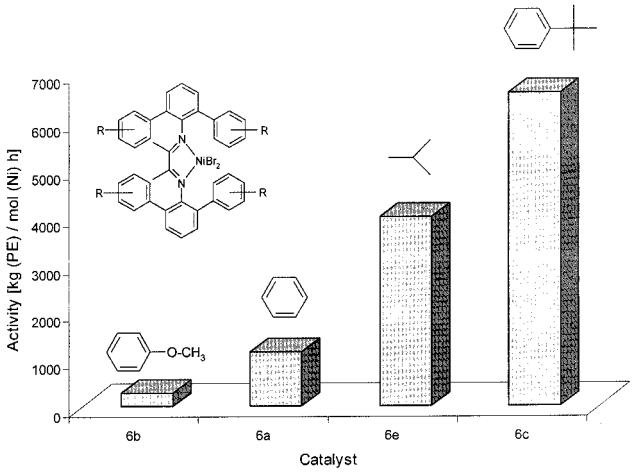

Figure 3. Comparison of the catalyst activities.

Conclusions

The family of sterically crowded 4-diaza-2,3-dimethylbutadiene ligands that contain the new 2,6-di(phenyl)aniline building blocks (e.g., **3a**−**d**) is easily accessible in good yields. The ligand **3c**, which carries bulky 2,6-di(4-*tert*-butylphenyl)aniline fragments, leads to chiral stereorigid complexes (e.g., **4**−**6c**) showing C_2-symmetry. The pronounced steric influence of this ligand on the metal center results in a distinct distortion of the square-planar coordination geometry. Interestingly, this is in agreement with the fact that the Ni(II) compound **6c**/MAO gives the most active catalyst system of the present study and produces the highest molecular weight products.

(17) We had problems controlling the reaction temperature due to these unexpected high activities and switched therefore to a 2 L reactor setup, equipped with an internal cooling device. However, the activity values given in Table 4 can only be first estimates due to the rapid precipitation of the high molecular weight polymers. We suggest that the real values are substantially higher (cf. section on hydrogen addition).

(18) Deng, L.; Margl, P.; Ziegler, T. *J. Am. Chem. Soc.* **1997**, *119*, 1094. (b) Deng, L.; Woo, T. K.; Cavallo, L.; Margl, P.; Ziegler, T. *J. Am. Chem. Soc.* **1997**, *119*, 6177.

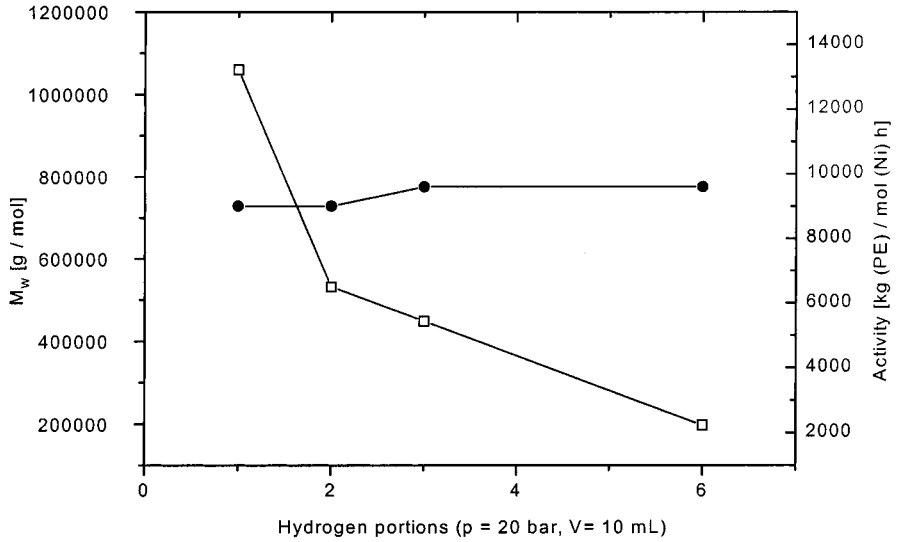

Figure 4. Dependence of molecular weight and activity on the hydrogen concentration.

Table 2. Summary of Crystal Data, Data Collection, and Structure Refinement Parameters

	4a	4b	4c
empirical formula	$C_{40}H_{32}Cl_2N_2Pd$	$C_{52}H_{50}Cl_{18}N_2O_5Pd$	$C_{56}H_{64}Cl_2N_2Pd$
fw	717.98	1527.44	942.39
cryst color and form	red prism	yellow prism	red prism
cryst system	orthorhombic	triclinic	orthorhombic
space group	$P2_12_12$	$\bar{P}1$	*Pbca*
a (Å)	13.245(3)	12.163(1)	21.477(4)
b (Å)	13.259(3)	12.859(2)	16.216(3)
c (Å)	9.296(5)	23.641(3)	28.591(6)
α (deg)	90	95.99(1)	90
β (deg)	90	99.65(2)	90
γ (deg)	90	117.47(1)	90
V (Å^3)	1632.5(10)	3163.4(6)	9957(3)
Z	2	2	8
D_C (Mg/m^3)	1.461	1.604	1.257
abs coeff μ (mm^{-1})	0.764	1.100	0.517
F(000)	732	1552	3952
cryst size (mm)	0.30 × 0.25 × 0.24	0.42 × 0.23 × 0.15	0.38 × 0.37 × 0.26
scan mode	$\omega/2\theta$		ϕ-scan
θ_{max} (deg)	24.99	25.90	25.25
index ranges	$0 \le h \le 15$	$-14 \le h \le 14$	$-25 \le h \le 25$
	$0 \le k \le 15$	$-15 \le k \le 15$	$-19 \le k \le 19$
	$0 \le l \le 11$	$-29 \le l \le 28$	$-34 \le l \le 34$
no. of unique reflns	1639	11 460	8053
no. of obsd reflns [$I > 2\sigma(I)$]	1428	24 195	4756
no. of params	230	704	550
goodness-of-fit on $S(F^2)$[a]	1.105	0.998	0.924
final *R* indices [$I > 2\sigma(I)$][b]	R1 = 0.0818, wR2 = 0.2314	R1 = 0.0548, wR2 = 0.1471	R1 = 0.0858, wR2 = 0.2037
R indices (all data)[b]	R1 = 0.0929, wR2 = 0.2392	R1 = 0.0771, wR2 = 0.1570	R1 = 0.1453, wR2 = 0.2337
largest diff peak and hole (e/Å^3)	1.649 and −0.618	3.021 and −1.286	2.722 and −0.929

[a] $S = [\sum[w(F_o^2 - F_c^2)^2]/(n-p)]^{1/2}$, where *n* is the number of reflections and *p* is the number of refined parameters. [b] $R1 = \sum||F_o| - |F_c||/\sum|F_o|$; $wR2 = [\sum[w(F_o^2 - F_c^2)^2]/\sum wF_o^4]^{1/2}$.

Ligand **3c** was designed to create chirality—and in particular C_2-symmetry—in polymerization active diimine complexes. Meso structures, like those known in metallocene chemistry, are unlikely to exist with **3c**, due to the high steric demand of the *tert*-butyl substituents. Future work will show if these chiral catalysts that bear late transition metal centers can control the stereochemistry of 1-olefin homo- and copolymerization reactions.

Experimental Section

General Procedures. Complex synthesis was performed under dry argon atmosphere using conventional Schlenk techniques. All Ni(II) complexes were generated by in situ reactions of the ligand with $(DME)NiBr_2$ in toluene and activated using MAO as cocatalyst. Hydrocarbons and ether solvents were dried by distillation from $LiAlH_4$, and methylene chloride was distilled from CaH_2. Aryl bromides, magnesium turnings, trimethylborate, phenylboronic acid, 2,6-dibromoaniline, 2,3-butanedione, $PdCl_2$, $(DME)NiBr_2$, and $Sn(CH_3)_4$ were used as received from Fluka, Merck, and Aldrich. $(C_6H_5CN)_2PdCl_2$,[20] $(COD)PdCl_2$,[21] (COD)PdMeCl,[12] $(Ph_3P)_4Pd(0)$,[22]

(19) Margl, P.; Deng, L.; Ziegler, T. *Organometallics* **1999**, *18*, 5701. (b) Small, B. L.; Brookhart, M.; Bennett, A. M. A. *J. Am. Chem. Soc.* **1998**, *120*, 4049. (c) Britovsek, G. J. P.; Gibson, V. C.; Kimberley, B. S.; Maddox, P. J.; McTavish, S. J.; Solan, G. A.; White, A. J. P.; Williams, D. J. *Chem. Commun.* **1998**, 849.

(20) Doyle, J. R.; Slade, P. E.; Jonassen, H. B. *Inorg. Synth.* **1960**, *6*, 218.

(21) Drew, D.; Doyle, J. R. *Inorg. Synth.* **1972**, *13*, 52.

Chart 3

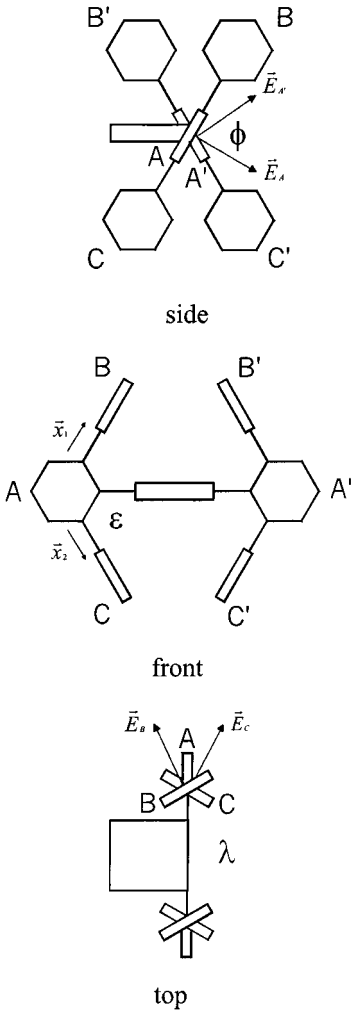

		4a	4b	4c
ε	$\vec{x}_1$, $\vec{x}_2$	127.0	125.6	138.6
ϕ	$\vec{E}_A$, $\vec{E}_{A'}$	7.5	27.8	51.4
λ	$\vec{E}_B$, $\vec{E}_C$	75.4	81.6	43.3

Table 3. Ethene Polymerization Results with Palladium Monomethyl Complexes

run[a]	catalyst	amount[b]	yield[c]	M_w[d]	M_w/M_n	T_m[e]
1	**5a**	50	1.0	11 400	1.6	66
2	**5b**	25	0.7	11 600	1.8	78
3	**5c**	25	0.3	13 500	2.0	116

[a] $p(C_2)$ 30 bar, reaction time 60 min. [b] [μmol]. [c] [g]. [d] [g mol^{-1}]. [e] [°C].

$Na[(3,5\text{-}(CF_3)_2C_6H_3)_4B]$,[23] and 2,3-butanedionebis(isopropylphenylimine)[6] were prepared according to literature procedures.

Methylalumoxane was purchased from Witco and toluene for the polymerization reactions from Merck.

All compounds were analyzed by ^1H and ^{13}C NMR on Bruker AC200 or AMX 500 spectrometers at ambient temperature and were referenced to TMS. Mass spectra were acquired with Finnigan (SSQ 7000) and Varian (MAT-711) instruments. Elemental analyses were determined in the Microanalytical Laboratory of the University of Ulm.

(22) Coulson D. R. *Inorg. Synth.* **1972**, *13*, 121.

X-ray Crystallography. The structures of the complexes **4a**−**c** were determined from single-crystal X-ray data. The crystallographic data are given in Tables 1 and 2. Crystals suitable for X-ray investigations were obtained from a tetrachloroethane solution (**4a**, **4b**) and from an acetonitrile solution (**4c**).

The structures of **4a** and **4c** were solved by direct methods (SHELXS-97)[24] and refined by a least-squares method based on F^2 with all reflections (SHELXL-97).[25] All non hydrogen atoms were refined anisotropically; the hydrogens were placed in calculated positions.

The structure of **4b** was resolved by the Patterson method (SHELXS-86).[26] The composition of the crystals was **4b**·$4C_2H_2Cl_4$·H_2O. The high chlorine content of the product was confirmed by an EDX measurement.

In compound **4a** the molecule exists in two orientations. The best fit was obtained with site occupation factors of 0.80 (main component) and 0.20. The structure could satisfactorily be solved and refined only in space group $P2_12_12$.

In **4b** several Cl atoms of the molecules of crystallization exhibit rather high thermal parameters. This indicates some disorder in this part of the crystal structure. The highest peak in the final ΔF map is 3.02 e Å^{-3}. It is situated 1.41 Å away from Cl(18).

Several slightly twinning crystal specimens were tested for **4c** using both conventional four-circle and CCD diffractometers at different temperatures, which varied from room temperature down to 193 K. The best result was obtained at room temperature with a CCD device. The atoms of *tert*-butyl groups have more than one orientation, but attempts to divide the butyl groups into partly occupied positions were unsuccessful.

Tables of crystal data, atomic parameters, bond lengths, and angles for **4a**−**c** have been deposited with the Cambridge Crystallographic Data Center. The deposition numbers are CCDC 154032 (**4a**), CCDC 154685 (**4b**), and CCDC 154033 (**4c**).

General Procedure for the Synthesis of Boronic Acids (Modified from Ref 9). In a 500 mL Schlenk flask, a solution of 1 equiv of the aryl bromide was added dropwise to 1.023 equiv of magnesium turnings. The resulting Grignard solution was filtered and added slowly dropwise with stirring to a calculated amount of trimethyl borate in ether at such a rate that the temperature did not rise above −70 °C. Therefore the flask was cooled using a dry ice/2-propanol mixture. The suspension was allowed to come to room temperature overnight. Then the mixture was added with stirring to ice (100 g) and concentrated sulfuric acid (5 mL). After stirring for 30 min, the mixture was shaken repeatedly with ether. Evaporation of the dried (Na_2SO_4) etheral extract gave a solid which could be filtered and dried in vacuo.

4-Methoxyboronic Acid (1b). 4-Bromoanisol (20.0 mmol, 37.4 g); magnesium (26.0 mmol, 6.3 g); trimethylborate (26.0 mmol, 2.7 g).

1b: white solid; yield 28.8 g (95%). ^1H NMR (methanol-d_4): δ 3.71 (s, $-OCH_3$, 3H), 6.82 (d, arom, 2H), 7.66 (d, arom, 2H). ^{13}C NMR (methanol-d_4): δ 55.65; δ 114.27; 136.75; 137.69; 163.06. Anal. Calcd for $C_7H_9O_3B$: C, 55.63; H, 5.97. Found: C, 54.98; H, 6.08.

4-*tert*-Butylboronic Acid (1c). 1-Bromo-4-*tert*-butylbenzene (117.3 mmol, 25.0 g); magnesium (117.3 mmol, 2.85 g); trimethylborate (142.3 mmol, 14.78 g).

1c: white solid; yield 21.1 g (83.4%). ^1H NMR (methanol-d_3): δ 1.34 (s, *t*-Bu, 9H), 7.42 (d, arom, 2H), 7.68 (d, arom,

(23) Grant B.; Volpe A. F., Jr.; Brookhart M. *Organometallics* **1992**, *11*, 3920.

(24) Sheldrick, G. M. *SHELX97*, Programs for Crystal Structure Analysis (Release 97-1); University of Göttingen: Germany, 1997.

(25) Sheldrick, G. M. *SHELXL97*, Program for the Refinement of Crystal Structures; University of Göttingen: Germany, 1997.

(26) Sheldrick, G. M. *SHELXS86*, Program for Crystal Structure Solution; University of Göttingen: Germany, 1986.

Table 4. Ethylene Polymerizations with Nickel Catalysts/MAO

run[a]	$p(C_2)$[b]	catalyst	amount[c]	time[d]	yield[e]	activity[f]	M_w[g]	M_w/M_n	T_m[h]
1	10	**6a**	0.04	30	23	1200	n.s.		133
2	30	**6a**	0.04	15	60	6000	n.s.		134
3	10	**6c**	0.02	15	33	6600	4.5	1.3	130
4	30	**6c**	0.02	15	101	20 200	n.s.		130
5	10	**6b**	0.04	120	22	300	n.s.		132
6	10	**6e**	0.02	15	20	4000	3.89	2.3	92

[a] Experimental conditions: 2 L steel reactor, 800 mL of toluene, cocatalyst MAO (Al:Ni ≈ 500). [b] [bar]. [c] [mmol]. [d] [min]. [e] [g]. [f] [g(PE) (mol(Ni) h)$^{-1}$]. [g] [10^6 g mol^{-1}]. [h] [°C].

Table 5. Ethene Polymerization Reactions with 6c after Hydrogen Addition

run[a]	$c(H_2)$[b]	yield[c]	activity[d]	M_w[e]	M_w/M_n	T_m[f]
1	1	45	9000	1 060 000	3.1	135
2	2	45	9000	532 000	2.9	134
3	3	49	9600	449 000	3.0	135
4	6	49	9600	197 000	3.0	136

[a] Experimental conditions: 2 L steel reactor, 800 mL of toluene, cocatalyst MAO (Al:Ni ≈ 500), *n*(catalyst) 0.02 mmol, $p(C_2)$ 10 bar, reaction time 15 min. [b] H_2 addition: pressure buret (10 mL, 20 bar portions). [c] [g]. [d] [kg(PE) (mol(Ni) h)$^{-1}$]. [e] [g mol^{-1}]. [f] [°C].

2H). ^{13}C NMR (methanol-d_3): δ 31.95; 35.79; 125.71; 135.02; 154.51. Anal. Calcd for $C_{10}H_{15}BO_2$: C, 67.46; H, 8.49. Found: C, 66.98; H, 8.39.

3,5-Dimethylboronic Acid (1d). 5-Bromo-*m*-xylene (137.1 mmol, 25.38 g); magnesium (135.1 mmol, 3.33 g); trimethylborate (162.1 mmol, 16.84 g).

1d: white solid; yield 17.59 g (85.6%). ^{1}H NMR (methanol-d_3): δ 7.04 (s, arom, 2H), δ 6.69 (s, arom, 1H), δ 1.96 (s, $-CH_3$, 6H). ^{13}C NMR (methanol-d_3): δ 22.55; 133.62; 133.77; 134.03; 138.87. Anal. Calcd for $C_8H_{11}BO_2$: C, 64.07; H, 7.39. Found: C, 64.31; H, 7.24.

General Procedure for the Synthesis of the Terphenylamines (Modified from Ref 8). In a 1 L Schlenk flask 1 equiv of 2,6-dibromobenzene and [$Pd(PPh_3)_4$] (12 mol %) were dissolved in 200−240 mL of benzene. A solution of 3 equiv of the boronic acid in ethanol and an aqueous 2 M Na_2CO_3 solution (6 equiv) were added to the flask, which then was connected with a reflux condenser and flushed with argon. The reaction mixture was refluxed for the given reaction time. After that, the organic layer was separated and the amine precipitated as hydrochloride or hydrobromide salt by addition of 20 mL of HCl (**3a**,**b**) or HBr (**3c,d**). The precipitate was filtered off and washed with *n*-pentane.

In a 1 L flask, the desired amount of the salt was suspended in ether, and 2 M Na_2CO_3 solution was added slowly under vigorous stirring until the precipitate vanished. The organic layer was dried over Na_2SO_4 and the solvent evaporated until the amine began to crystalize. The product was filtered and dried in vacuo.

Terphenylamine (2a). 2,6-Dibromaniline (24.0 mmol, 6.02 g); $Pd(PPh_3)_4$ (3.0 mmol, 3.88 g); phenylboronic acid (72.0 mmol, 8.80 g); Na_2CO_3 (144.0 mmol); reaction time: 24 h.

2a: white solid; yield 5.58 g (95%). ^{1}H NMR ($CDCl_3$/TMS): δ 3.75 (s, $-NH_2$, 2H), 6.78 (t, arom, 1H), 7.22 (d, arom, 2H), 7.27 (t, arom, 2H), 7.37 (t, arom, 4H), 7.43 (t, arom, 4H). ^{13}C NMR: ($CDCl_3$/TMS): δ 118.07, 127.20, 127.87, 128.79, 129.28, 129.71, 139.71, 140.74. Anal. Calcd for $C_{18}H_{15}N$: C, 88.33; H, 6.16; N, 5.71. Found: C, 88.05; H, 6.15; N, 5.28.

4-Methoxyterphenylamine (2b). 2.6-Dibromoaniline (28.0 mmol, 7.15 g); $Pd(PPh_3)_4$ (3.4 mmol, 3.91 g); *p*-methoxyboronic acid (84.0 mmol, 12.9 g); Na_2CO_3 (168.0 mmol); reaction time: 50 h.

2b: white solid; yield 8.2 g (95%). ^{1}H NMR ($CDCl_3$/TMS): δ 3,73 (s, $-O-CH_3$, 12H), 6,74 (t, arom, 2H), 6,87 (d, arom, 8H), 6,97 (d, arom, 4H), 7.32 (d, arom, 8H). ^{13}C NMR ($CDCl_3$/TMS): δ 55.30; 114.25; 118.09; 127.60; 129.52; 130.43; 132.07; 141.19; 158.82. Anal. Calcd for $C_{20}H_{19}NO_2$: C, 78.70; H, 6.22; N, 4.59 Found: C, 78.58; H, 6.24; N, 4.59.

4-*tert*-Butylterphenylamine (2c). 2,6-Dibromoaniline (27.4 mmol, 6.87 g); $Pd(PPh_3)_4$ (3.28 mmol, 3.80 g); *p*-*tert*-butylboronic acid (82.2 mmol, 14.6 g); Na_2CO_3 (164.4 mmol); reaction time 72 h.

2c: white solid; yield 5.5 g (56%). ^{1}H NMR (acetone-d_6): δ 1.40 (s, *tert*-butyl, 18H), 6.83 (t, arom, 1H), 7.05 (d, arom, 2H), 7.48 (d, arom, 4H), 7.53 (d, arom, 4H). ^{13}C NMR (acetone-d_6): δ 31.95; 35.33; 118.72; 126.72; 128.54; 129.88; 130.54; 138.30; 142.51; 150.82. Anal. Calcd for $C_{26}H_{31}N$: C, 87.34; H, 8.74; N, 3.92 Found: C, 87.12; H, 8.71; N, 3.89.

General Procedure for the Synthesis of the Diimine Ligands. In a 250 mL flask 2.2 equiv of the terphenylamine compound were dissolved in benzene, and a catalytic amount of *p*-toluenesulfonic acid monohydrate was added. Then 1 equiv of 2,3-butanedione was added dropwise by syringe with stirring. After that, the flask was connected with a water separator and a reflux condenser. After refluxing the mixture for the needed reaction time, the solvent was evaporated in vacuo. The crude product was dissolved in warm methylene chloride, and the ligand was precipitated by addition of methanol, filtered, and dried in vacuo.

2,3-Butanedionebis(terphenylimine) (3a). Terphenylamine (**2a**) (12.1 mmol, 2.97 g); 2,3-butanedione (5.5 mmol, 0.48 mL); benzene (75 mL); reaction time 12 h.

3a: yellow crystals; yield 2.53 g (85%). ^{1}H NMR ($C_2D_2Cl_4$): δ 1.37 ($-CH_3$, 6H), 6.9−7.4 (m, arom, 26H). ^{13}C NMR ($C_2D_2Cl_4$): δ 16.45; 124.26; 126.91; 127.94; 129.03; 129.58; 131.13; 139.71; 146.23; 167.07. Anal. Calcd for $C_{40}H_{32}N_2$: C, 88.85; H, 5.97; N, 5.18 Found: C, 88.27; H, 5.97; N, 5.13.

2,3-Butanedionebis(4-methoxyterphenylimine) (3b). *p*-Methoxyterphenylamine (**2d**) (14.7 mmol, 4.5 g); 2,3-butanedione (8.1 mmol, 0.71 mL); benzene (180 mL); reaction time 60 h.

3b: yellow crystals; yield 4.0 g (83%). ^{1}H NMR ($C_2D_2Cl_4$): δ 1.54 (s, $-CH_3$, 6H), 3.88 (s, $-O-CH_3$, 12H), 6.80 (d, arom, 8H), 7.20 (m, arom, 10H), 7.28 (d, arom, 4H). ^{13}C NMR ($C_2D_2Cl_4$): δ 16.66; 55.34; 113.53; 124.03; 129.19; 130.14; 130.97; 132.57; 146.21; 158.54; 167.35. Anal. Calcd for $C_{44}H_{40}N_2O_2$: C, 79.98; H, 6.10; N, 4.24 Found: C, 78.98; H, 6.04; N, 4.04.

2,3-Butanedionebis(4-*tert*-butylterphenylimine) (3c). 4-*tert*-Butylterphenylamine (**2c**) (7.7 mmol, 2.45 g); 2,3-butanedione (4.24 mmol, 0.38 mL); benzene (75 mL); reaction time 72 h.

3c: yellow crystals; yield 1.8 g (61%). ^{1}H NMR ($C_2D_2Cl_4$): δ 1.23 ($-CH_3$, 6H), 1.38 (*tert*-butyl, 36H), 7.1−7.5 (m, arom, 22H). ^{13}C NMR ($C_2D_2Cl_4$): δ 17.88; 31.55; 34.51; 124.14; 124.80; 128.91; 129.46; 131.60; 137.27; 145.69; 149.55; 167.92. Anal. Calcd for $C_{56}H_{64}N_2$: C, 87.91; H, 8.43; N, 3.66 Found: C, 87.23; H, 8.40; N, 3.44.

Dichloro(2,3-butanedionebis(terphenylimine))palladium(II) (4a). In a 100 mL Schlenk flask 457 mg (1.6 mmol) (COD)$PdCl_2$ was dissolved in 50 mL of methylene chloride. After addition of 900 mg (1.66 mmol) of ligand **3a**, the mixture was stirred for 3 days, while the color of the solution changed from yellow to dark orange. The solvent then was reduced in

vacuo, and the complex was precipitated by addition of ether. Finally the product was filtered, washed with ether and *n*-pentane, and dried in vacuo.

4a: yellow powder; yield 940 mg (82%). ^{1}H NMR ($C_2D_2Cl_4$): δ 1.43 (s, $-CH_3$, 6H); 7.07−7.31 (m, arom, 26H). ^{13}C NMR ($C_2D_2Cl_4$): δ 16.52, 124.42, 126.93, 127.93, 128.97, 129.56, 131.20, 139.53, 145.82, 167.21. Anal. Calcd for $C_{40}H_{32}Cl_2N_2$-Pd: C, 66.85; H, 4.46; N, 3.89 Found: C, 66.95; H, 4.43; N, 3.66.

Dichloro(2,3-butanedionebis-4-methoxyterphenylimine))palladium(II) (4b). In a 500 mL Schlenk flask containing 1.15 g (3.0 mmol) of $(PhCN)_2PdCl_2$, 250 mL of methylene chloride and 2.0 g (3.05 mmol) of ligand **3b** were added. After a few minutes the color of the reaction mixture changed to dark red. The mixture was stirred for 72 h at room temperature. Then the methylene chloride was removed in vacuo until only about 15 mL of the solvent remained. Then the complex was precipitated by addition of 50 mL of *n*-pentane. The solvents were removed via filtration, and the product was washed with *n*-pentane and dried in vacuo.

4b: orange powder; yield 2.44 g (97%). ^{1}H NMR ($C_2D_2Cl_4$): δ 1.55 (s, $-CH_3$, 6H); 3.91 (s, −O−CH3, 12H); 6.82 (d, arom, 8H); 7.19 (d, arom, 4H); 7.44 (m, arom, 10H). ^{13}C NMR: (C_2D_2-Cl_4): δ 21.21; 55.46; 114.33; 128.55; 130.66; 131.02; 131.18; 135.00; 140.68; 159.03; 178.12. Anal. Calcd for $C_{44}H_{40}Cl_2N_2O_4$-Pd: C, 63.05; H, 4.81; N, 3.34 Found: C, 62.62; H, 4.87; N, 3.35.

Dichloro(2,3-butanedionebis-4-*tert*-butylterphenylimine))palladium(II) (4c). Following the procedure described for compound **4b**, 652 mg (1.7 mmol) of $(C_6H_5CN)_2PdCl_2$ and 1.43 g (1.86 mmol) of ligand **3c** were converted in 75 mL of methylene chloride to the palladium dichloro complex.

4c: dark orange powder; yield 1.36 g (85%). ^{1}H NMR (C_2D_2-Cl_4): δ 1.22 (s, $-CH_3$, 6H), 1.38 (s, $-CH_3$, 36H), 7.15 (d, arom, 8H), 7.23 (t, arom, 2H), 7.35 (t, arom, 12H). ^{13}C NMR (C_2D_2-Cl_4): δ 17.85, 31.54, 34.51, 124.11, 124.79, 128.9, 129.46, 131.59, 137.26, 145.71, 149.54, 167.89. Anal. Calcd for $C_{56}H_{64}$-Cl_2N_2Pd: C, 71.30; H, 6.79; N, 2.97. Found: C, 70.97; H, 6.86; N, 2.99.

Methylchloro(2,3-butanedionebis(terphenylimine))-palladium(II) (5a). Ether (75 mL) was added to a Schlenk flask containing 530 mg (2.0 mmol) of (COD)PdMeCl and a slight excess of ligand **3a** (1.13 g, 2.1 mmol). An orange precipitate began to form immediately upon mixing. The reaction mixture was stirred overnight, and the ether and free COD were removed via filtration. The product was washed with ether and dried in vacuo.

5a: orange powder; yield 1.03 g (74%). ^{1}H NMR ($C_2D_2Cl_4$): δ 0.65 (s, $-CH_3$, 3H); 1.53 (s, $-CH_3$, 3H), 1.57 (s, $-CH_3$, 3H), 7.09−7.49 (m, arom, 24H), 7.62 (d, arom, 3H). ^{13}C NMR (C_2D_2-Cl_4): δ 1.77; 20.23; 22.18; 126.45; 127.39; 127.69; 127.72; 128.45; 128.69; 128.81; 129.43; 130.96; 131.34; 134.26; 134.49; 138.42; 139.18; 140.91; 141.68; 169.95; 174.60. Anal. Calcd for $C_{41}H_{35}ClN_2Pd$: C, 70.57; H, 5.06; N, 4.01. Found: C, 70.57; H, 5.04; N, 4.05.

Methylchloro(2,3-butanedionebis-4-methoxyterphenylimine))palladium(II) (5b). In a 250 mL Schlenk flask 0.6 g (0.71 mmol) of compound **4b** was suspended in 120 mL of methylene chloride. $Sn(CH_3)_4$ (0.25 mL, 1.77 mmol) was added via syringe, and the reaction mixture was stirred at room temperature for 40 h. The resulting red solution was filtered and reduced to a volume of about 20 mL. The product was precipitated by addition of 150 mL of ether using an ice bath for cooling. The solvent was removed via filtration, and the complex was washed with ether and dried in vacuo.

5b: orange powder; yield 0.4 g (69%). ^{1}H NMR ($C_2D_2Cl_4$): δ 0.64 (s, Pd−CH_3, 3H); 1.40 (s, $-CH_3$, 3H); 1.42 (s, $-CH_3$, 3H); 3.84 (s, −O−CH_3, 6H); 3.85 (s, −O−CH_3, 6H); 6.68 (d, arom, 4H); 6.81 (d, arom, 4H); 7.17 (d, arom, 6H); 7.24 (d, arom, 2H); 7.31 (m, arom, 2H); 7.63 (d, arom, 4H). ^{13}C NMR (C_2D_2-Cl_4): δ 3.27; 21.36; 23.05; 56.75; 115.13; 115.48; 127.93; 128.84; 131.63; 132.26; 133.22; 135.11; 135.37; 142.36; 143.22; 160.05; 171.37; 176.07. Anal. Calcd for $C_{45}H_{43}ClN_2O_4Pd$: C, 66.10; H, 5.30; N, 3.42 Found: C, 65.86; H, 5.38; N, 3.38.

Methylchlororo(2,3-butanedione-bis-4-*tert*-butylterphenylimine))palladium(II) (5c). In a 250 mL Schlenk flask 0.8 g (0.84 mmol) of compound **4c** was dissolved in 80 mL of methylene chloride. After the addition of a catalytic amount of Et_3NH_4Cl, 0.3 mL (2.1 mmol) of $Sn(CH_3)_4$ was added via syringe, and the reaction mixture was stirred at room temerature for 40 h. The resulting orange solution was filteredand reduced to a volume of about 20 mL. The product was precipitated by addition of ether. Finally the solvent was removed via filtration, and the complex was washed with ether and dried in vacuo.

5c: orange powder; yield 0.542 g (70%). ^{1}H NMR (C_2D_2-Cl_4): δ 0.41 (s, $-CH_3$, 3H), 1.07 (s, $-CH_3$, 3H), 1.11 (s, $-CH_3$, 3H), 1.32 (d, $-CH_3$, 36H), 7.23−7.54 (m, arom, 22H). ^{13}C NMR ($C_2D_2Cl_4$): δ 7.86; 20,44, 21.53; 31.45; 31.48; 34.55; 34.61; 124.65; 125.12; 127.03; 127.88; 129.58; 130.10; 134.26; 134.64; 135.80; 136.55; 141.26; 141.43; 150.24; 150.80; 156.53; 171.13; 175.21. Anal. Calcd for $C_{57}H_{67}ClN_2Pd$: C, 74.18; H, 7.27; N, 3.04. Found: C, 73.95; H, 7.20; N, 3.01.

Synthesis of the Nickel Catalysts. The nickel complexes were performed in situ by reaction of the ligand with (DME)-$NiBr_2$ in toluene for 12 h. The resulting solutions were directly activated by addition of MAO and used for polymerizations.

Polymerization Reactions with Ethylene. Palladium Monochloro Compounds. The calculated amount of the catalyst was dissolved in methylene chloride (50 mL/100 mL steel reactor, 30 mL/50 mL steel reactor) under argon. Two equivalents of $NaB(Ar')_4$ was added, and the autoclave was pressurized with ethene. The pressure was kept constant during the reaction time. The polymerizations were stopped by pouring the reaction mixture into methanol. The polymers were filtered, washed with methanol, and dried in vacuo overnight. Polyethene was obtained in yields from 0.3 to 1.05 g.

Palladium Dichloro Compounds. Polymerizations were performed using the above-described procedure in a 50 mL steel autoclave, in which toluene, cocatalyst MAO, and the catalyst were fed under argon. The polymerizations were quenched by pouring the reaction mixture in acidified methanol. Polyethene was obtained in yields from 0.75 to 3.24 g.

Nickel Dibromo Compounds. A 2000 mL steel autoclave was charged with 800 mL of toluene under argon. In case of the hydrogen experiments, a pressure buret was repeatedly pressurized with hydrogen (V = 10 mL, p = 20 bar) and exhausted into the reactor until the desired hydrogen concentration was obtained. Then the reactor was pressurized with ethene. After the solution was saturated with monomer, the activated catalyst solution was injected into the autoclave via a pressure buret. The pressure was kept constant during the entire polymerization period. The polymerization reactions were stopped and treated as described above yielding 20−101 g of polyethene.

Polymer Analysis. The soluble polymers were analyzed by ^{1}H and ^{13}C NMR on a Bruker AC 200 or AMX 500 at 80 °C in $C_2D_2Cl_4$. Molecular weights were determined by a Waters 150 C ALC/GPC system in 1,2,4-triclorobenzene at 135 °C. DSC measurements were done using a Perkin-Elmer series 7 DSC instrument.

Acknowledgment. We are grateful to Prof. Dr. Markku Ahlgren, Department of Chemistry, University of Joensuu, Finland, for collecting the X-ray data of **4c**. We also wish to thank Prof. Ulf Thewalt, Section for X-Ray and Electron Diffraction, University of Ulm, for the structure solution of **4b**. Finally we are grateful to

the Bundesministerium für Bildung und Forschung (BMBF) as well as the BASF AG for generous financial support.

Supporting Information Available: Tables of crystallographic data, bond distances, bond angles, anisotropic displacement parameters, and complete atom coordinates and thermal parameters. This material is available free of charge via the Internet at http://pubs.acs.org.

OM010001F